Statistical Corrections to Numerical Prediction Equations[1,2]

ALAN J. FALLER AND DAVID K. LEE

Institute for Fluid Dynamics and Applied Mathematics and The Graduate Program for Meteorology, University of Maryland, College Park 20742

(Manuscript received 24 March 1975; in revised form 7 July 1975)

ABSTRACT

A procedure for statistical correction of numerical prediction equations at the end of each predictive time step is described and tested with a one-dimensional prediction model. The model equation is a modified Burgers equation that allows the formation of shocks, analogous to atmospheric fronts, and which contains a space and velocity-dependent source of energy to maintain the flow against dissipation. The detailed flow is calculated from a fine-grid numerical integration. Coarse-grid values, for testing a coarse-grid prediction scheme, are obtained by space-time averages.

Since the coarse-grid prediction equation cannot represent the sub-grid-scale motions, statistical corrections are added in the form of parametric terms as a pragmatic substitute for the missing sub-grid-scale effects. Tests with different versions of the model show that substantial improvement over the straightforward coarse-grid prediction can be obtained when the coefficients of appropriate parametric terms are determined by a multiple regression procedure.

1. Introduction

The goal of this research is to assess the effectiveness of correcting errors of numerical prediction by statistical corrections applied during each time step. The errors to which we address ourselves are those due to sub-grid-scale (SGS) effects or those due to improperly specified or omitted physical mechanisms. SGS errors are often divided into various categories such as those associated with truncation error, Reynolds stresses, unresolved physical processes, and unresolved boundary conditions, etc., but it should be recognized that in fact these are all part of the same effect due to a numerical grid that is coarse relative to many of the phenomena of interest. When one considers phenomena whose scales span the grid scale, for example, the distinction between truncation error and Reynolds stresses disappears.

The success of the statistical procedure, to be specified in detail below, will depend upon there being a significant statistical relation between the grid-scale variables and the SGS phenomena. Thus, in the atmosphere SGS phenomena such as fronts and general thunderstorm activity must be related to the larger-scale fields of motion, temperature, humidity, etc. Consequently, there is some hope of parameterizing their effects upon the large-scale circulation without specifying their details. Surely we are also interested in the details of frontal systems and thunderstorms, but these details require specific SGS information. We are concerned here not with the details of SGS phenomena, only with their effects upon the larger-scale flows that are calculable with the relatively coarse grid.

In certain cases of limited interest there now appear to be acceptable methods of incorporating SGS turbulence effects into numerical models provided that the grid-scale cut off lies within the inertial subrange. These methods (for example Leith, 1969) generally rely upon dimensional arguments. They appear to have been successfully employed in various two-dimensional (Crowley, 1970) and three-dimensional (Deardorff, 1970) turbulence models. However, such methods cannot at this time effectively take into account SGS phenomena whose scales span the grid scale and which may be described as organized SGS motions as opposed to turbulence.

Our method must be characterized as an empirical approach, since it depends upon the existence and use of historical data. The empirical calculation of an eddy coefficient of viscosity has certain similarities to our procedure but there are significant differences as well. These are: 1) more elaborate modifications of the dynamic equations are included; for example, modification of the advection by additional parametric terms; 2) the added parametric terms are integrated

[1] The research reported here has been supported in part by the National Science Foundation under Grants GA-26028 and DES74-24132. Computer time for Graduate Student Research was provided by the Computer Science Center of the University of Maryland.

[2] Publication No. 119 from the Graduate Program for Meteorology.

into the numerical method in an attempt to optimize predictions; and 3) to account for spatial and temporal variations of the dynamics, the empirical coefficients of the added terms may be taken as functions of space and time insofar as the historical data and computer time may permit.

It will be recognized immediately that the proposed procedure is one that could become very complex, far more so than most of the statistical or semi-statistical forecasting procedures that are currently anticipated in meteorology. The atmosphere contains such a variety of SGS phenomena and there are so many parameters that might be judged to be significant for SGS effects that an attempt at direct application to the atmosphere would probably be very discouraging. Therefore, we have elected to develop and test the proposed method first with a series of relatively simple models.

2. The general procedure

To introduce the method, we first briefly outline the sequence of operational steps without detailed explanation or example. These are:

1) Obtain historical data on a space-time grid appropriate to the coarse space-time grid to be used for prediction. These historical data are to be referred to as the "correct data" (e.g., U_c) in comparison with predicted values (e.g., U_p) even though it is recognized that the historical data may be subject to observational or interpolational error. By way of example for the atmosphere, if the 500 mb height field were to be predicted with a time step of one hour, to obtain the "correct data" at intervals of one hour it would be necessary to make time interpolation of the observed height fields that are normally available every 12 h.

2) Using a numerical model with coarse-grid intervals Δx and Δt, make a large number of one-time-step (OTS) predictions starting from various sets of the correct data obtained in Step 1. The numerical model used for these predictions will be referred to as the FIDI model.

3) Compare the OTS predictions with the correct data. For each OTS prediction and at each grid point determine an OTS error as the difference between the correct datum and the predicted value, e.g., $E=U_p-U_c$.

4) Select provisional parametric terms (P's) to relate SGS effects to the coarse-grid variables. These P terms are evaluated in finite-difference form using the correct data for all space-time grid points at which OTS predictions have been made and for which OTS errors have been calculated.

5) Make a multiple correlation of the P's evaluated in Step 4 with the OTS errors calculated in Step 3. Screen the P's for independence and statistical significance. Having selected a set of optimum P's obtain the multiple-regression coefficients for estimating E from the P's.

6) Modify the numerical model used in Step 2 (the FIDI model) by adding the regression equation obtained in Step 5. The modified numerical prediction equation is called the STAT model. The STAT model thus consists of the FIDI prediction plus a statically determined error correction at each time step.

7) Test the effectiveness of the STAT model as compared to the FIDI model by making several extended predictions starting with identical correct data in each model. Using the correct data for verification, compare the rms errors of prediction of the STAT and FIDI models, or some other suitable measure of predictability.

There are many alternatives to be considered in carrying out this procedure. Beginning with Step 1 the values of Δx and Δt must be fixed and the historical data (the correct data) must be identified. Applied to the atmosphere, if direct observations existed at the selected space-time grid points these could represent the correct data. We prefer some type of smoothed data rather than point values and in these studies have chosen space-time mesh-box averages. It is important to note that the method relies on the consistent use of the same Δx and Δt and consistent analysis of the historical data throughout the study and for future predictions with the STAT model.

In Step 2 a suitable FIDI prediction equation must be selected, and the same model and numerical methods must be used throughout the study. In Step 3 alternatives to the determination of errors by one-step predictions do exist, but the evaluation of errors after several time steps, for example, seems to lead to difficulties of interpretation or cumbersome statistical and numerical problems.

The selection of the provisional P's in Step 4 offers a wide range of possibilities and hazards, the more so as the complexity of the dynamical system increases and as the SGS processes become more important for the large-scale dynamics. In the present study the principal parametric effects that we have found useful represent, in essence, simple modifications of the advection and diffusion processes. But, in any dynamical system, if significantly different values of Δx and Δt are chosen the SGS effects will change accordingly and different P's may be required for optimum results.

The selection of the "significant" P's from the original provisional set by multiple correlation methods as in Step 5 has several possible pitfalls. To avoid the undesirable effects of interdependent P's the concepts and methods of empirical orthogonal functions might be found useful, but this has not been attempted in this study. Perhaps a more serious problem is that because of cumulative effects in an extended numerical prediction it can happen that some P's that may have significant correlations with OTS errors should not be included in the STAT equation.

Because of these and other uncertainties we have elected to conduct initial tests with a simplified dynamical system. This avoids many of the complexities

that will be found in direct application to the atmosphere such as the problem of acquiring a suitable set of historical data. Our model system is a modified one-dimensional Burgers (1974) equation in finite-difference form. The use of this relatively simple equation limits the number and types of dynamical interactions that may occur. But this restriction also allows us to calculate a large body of "correct data" with a fine-grid numerical calculation rather than relying upon observations of a physical system. The fine grid is capable of resolving small scales of motion that become the SGS effects when the coarse grid is used. In these studies the coarse-grid correct values are determined by space-time mesh-box averaging of the fine-grid data.

3. The model equation

The simple one-dimensional Burgers equation, $u_t+uu_x=\nu u_{xx}$, has been modified with an additional dissipative term and a source term to become

$$u_t+uu_x=\nu u_{xx}-ku+S(x,t,u) \qquad (1)$$

where $u=dx/dt$, ν is the viscosity, k is a dissipation constant, $S(x,t,u)$ is a source function for u that is used to overcome the dissipative loss of kinetic energy, and subscripts denote partial differentiation. This equation retains a significant nonlinear effect in uu_x and has the property that by elimination of the usual pressure term (in essence, assuming a fluid of infinite compressibility) the flow can develop strong discontinuities analogous to shocks. For our purposes these shocks may be thought of as similar to atmospheric fronts and are the significant SGS phenomena in our idealized system.

For an introduction to the characteristics of the Burgers equation please refer to Fig. 1, which illustrates the development and initial dissipation of a shock starting from the condition $u=0.5(1+\sin 2\pi x)$ and with a vanishingly small viscosity, $\nu\rightarrow 0$. This development in time is a simple graphical solution. Note that since $u=dx/dt$, in a given time interval Δt an element of fluid with $u>0$ moves to the right a distance $\Delta x=u\Delta t$, and an element on the x axis with $u=0$ remains fixed until the effect of viscosity is felt. With $\nu\rightarrow 0$ there is no viscous effect until infinitely sharp gradients occur as

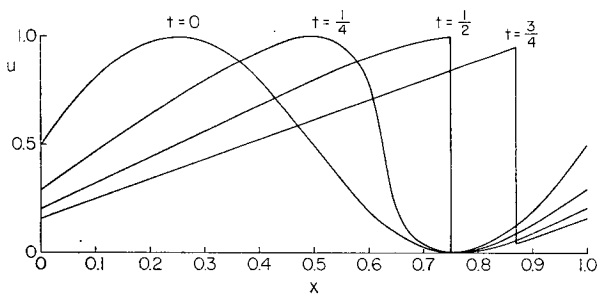

FIG. 1. An example of the development of flow with the Burgers equation starting from the initial conditions $u=0.5(1+\sin 2\pi x)$ and with $\nu\rightarrow 0$.

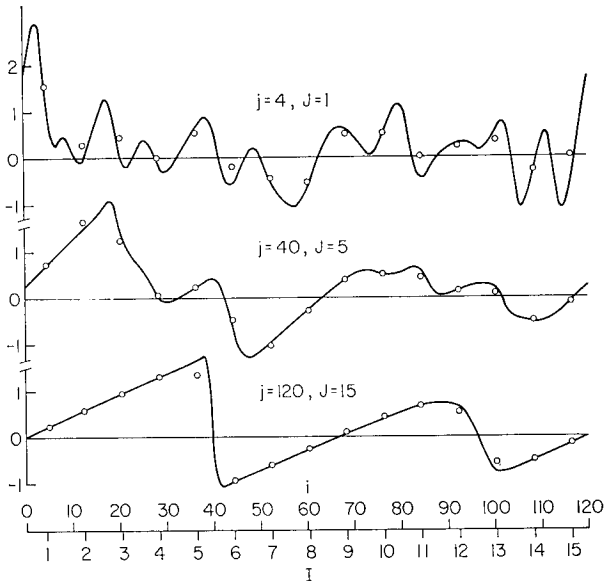

FIG. 2. The time development of the flow in Model I. Continuous curves indicate the fine grid calculations for time steps j at 120 i points. Indicated points are the space-time averaged values for the nearly corresponding coarse-grid time steps J at the 15 coarse-grid I points.

in the later stages of the development. Analytical solutions of the Burgers equation for a wide variety of initial conditions and applications have been analyzed and catalogued by Benton and Platzman (1972). The interested reader also may wish to refer to the interesting analysis of statistical problems related to the one-dimensional equation by Burgers (1974).

While we would not overemphasize the analogy between discontinuities occurring with the Burgers equation and atmospheric fronts, we will make occasional reference to comparative time and space scales so that eventual application to atmospheric problems will remain in sight as our ultimate objective. As a first comparison it is interesting to note that the time required for the formation of the shock in Fig. 1, from the initial sine wave, is comparable to the time one might expect for the formation of atmospheric fronts starting with a long-wave pattern. In the example of Fig. 1, this time is simply $T=L/2\Delta u$ where $L=1$ is the wavelength and $\Delta u=1$ is the difference between the maximum and minimum values of u. Choosing as an atmospheric counterpart $L=5000$ km and $u=20$ m/s we obtain $T=1.45$ days.

With a finite viscosity the wave of Fig. 1 would dissipate from the beginning and the shock would be of finite width rather than being infinitely thin as in the example. Figure 2 illustrates the development of a flow from a more complex initial state made up from a sum of several periodic waves and with a source $S(x,t,u)$ (to be specified in Section 5). As was the case in Fig. 1, and in all subsequent examples, the flow is taken to be periodic with the fundamental wavelength L. The de-

tailed time development represented in Fig. 2 was numerically carried out with space and time intervals δx and δt sufficiently small to accurately represent the smallest scales of the motion. Therefore, we refer to such a flow as the "true fine-grid" flow. In the same figure we have indicated the corresponding space-time-averaged values, averaged over discrete intervals $\Delta t=8\delta t$ and $\Delta x=8\delta x$. Although these averages smooth out features of the fine-grid flow, they are derived from the true fine-grid data and therefore are the true-average values, our "correct data" as described above. Referring back to Steps 1–7 in Section 2, these correct data are used: 1) to initiate the OTS predictions, 2) to determine the OTS errors, 3) to calculate the P's for correlation with the errors, 4) to initiate the extended predictions with both the FIDI and STAT models, and 5) to evaluate the predictive capabilities of the FIDI and STAT coarse-grid models.

4. Numerical methods and related model conditions

In both the fine-grid and the coarse-grid calculations we have used straightforward centered spatial differences for both the advective and diffusive terms with the advective term in the form $(u^2/2)_x$. Letting $x=i\delta x$ (or $I\Delta x$) and $t=j\delta t$ (or $J\Delta t$) where i, j, δx and δt refer to fine-grid calculations and I, J, Δx, and Δt refer to coarse-grid calculations, we have used throughout:

$$[(u^2/2)_x]_{i,j}\simeq[(u^2/2)_{i+1,j}-(u^2/2)_{i-1,j}]/2\delta x$$

and

$$(u_{xx})_{i,j}\simeq(u_{i+1,j}-2u_{i,j}+u_{i-1,j})/\delta x^2.$$

For time stepping we have used a simple forward step followed by one or more iterations to approximate an implicit solution. Thus, representing Eq. (1) (omitting S) by $u_t=F(u)$, a forward step followed by n iterations is specified by

$$u^{n+1}_{i,j+1}=u_{i,j}+\delta t\left[\frac{F(u_{i,j})+F(u^n_{i,j+1})}{2}\right]$$

with $u^0_{i,j+1}=u_{i,j}$. (2)

In general, our value of δt was sufficiently small that $n=1$ gave satisfactory results although larger values of n were occasionally used for comparative purposes or greater accuracy.

The source function $S(x,t,u)$, to be specified in detail below for each case, was always calculated at the end of the iteration from the values of $u^{n+1}_{i,j+1}$. Applying the source, the final value of u after one time step may be represented by

$$u_{i,j+1}=u^{n+1}_{i,j+1}+\delta t S(i,j+1,u^{n+1}_{i,j+1}). \quad (3)$$

A criterion that must be applied to avoid aliasing is that the viscosity should be large enough in some relative sense that scales of motion comparable to the grid scale should be very rapidly damped. This criterion is satisfied if the ratio of advective to dissipative terms for a wavelength of a few grid spacings is the order of unity. This leads to the criterion $\mathrm{Re}_t\equiv(\delta x\Delta u)/\nu$ (a turbulent or grid Reynolds number) $=0(1)$, where Δu is a difference between maximum and minimum speeds. We found that values up to about $\mathrm{Re}_t=3$ could be tolerated without introducing significant aliasing effects, effects that would otherwise distort a simple wave when it began to approach the anticipated viscously damped shock.

In all of the present studies the coarse-grid predictions made use of $\Delta t=8\delta t$ and $\Delta x=8\delta x$. Therefore, to avoid aliasing effects in the coarse-grid prediction as well as in the corresponding fine-grid calculations it was necessary to increase the viscosity by a factor of 8 for the coarse-grid calculations. This increase is analogous to the use of a large constant eddy-viscosity or comparable smoothing in atmospheric calculations to avoid aliasing.

Three models with different specifications for $S(x,t,u)$ but all based upon Eq. (1) will be discussed below. To avoid unnecessary variations between the three models the same numerical methods were used without variation once the methods described above had been selected. Initial conditions for the fine-grid calculations were specified in general by the Fourier series

$$u_{i,0}=\sum_{m=0}^{M}A_m\cos\frac{2\pi mi\delta x}{L}+B_m\sin\frac{2\pi mi\delta x}{L}, \quad (4)$$

where L is the fundamental periodic length.

For simplicity of comparative representation the fine-grid finite-difference prediction equation may be written

$$\frac{\delta u}{\delta t}=\nu\frac{\delta^2 u}{\delta^2 x^2}-\frac{\delta u^2/2}{\delta x}-ku+S(i,j+1,u) \quad (5)$$

and the coarse-grid prediction equation (FIDI model) is denoted by

$$\frac{\Delta U}{\Delta t}=N\frac{\Delta^2 U}{\Delta x^2}-\frac{\Delta U^2/2}{\Delta x}-kU+S(I,J+1,U). \quad (6)$$

After addition of the statistical terms, Eq. (6) becomes the STAT model

$$\frac{\Delta U}{\Delta t}=N\frac{\Delta^2 U}{\Delta x^2}-\frac{\Delta U^2/2}{\Delta x}-kU+S(I,J+1,U)+\sum C_l P_l. \quad (7)$$

The P_l terms are to be thought of as finite-difference forms of the parametric terms selected in the regression analysis. The coefficients C_l are the multiple regression coefficients, and in Eqs. (6) and (7) $N=8\nu$. In the STAT predictions the S and P terms are at first omitted while iteration of the remaining equation is performed. The S and P terms are then added to complete the time step.

We have restricted our P terms to only simple finite-difference representations involving grid points adjacent to the central point because the SGS effects are thought of as local phenomena. Although a variety of possible terms were tested, those that were found to be generally useful in this limited study are the restricted set:

$$P_1 = U^2_{I+1,J} - U^2_{I-1,J} \simeq (U^2/2)_x$$
$$P_2 = U_{I+1,J} - 2U_{I,J} + U_{I-1,J} \simeq U_{xx}$$
$$P_3 = U^4_{I+1,J} - U^4_{I-1,J} \simeq (U^4)_x$$
$$P_4 = U^2_{I+1,J} - 2U_{I+1,J}U_{I,J} + 2U_{I,J}U_{I-1.J} - U^2_{I-1,J} \simeq U_x U_{xx}$$

Since these terms are to be preceded by regression coefficients $C_1 - C_4$ it is not necessary to include factors such as $1/2\Delta x$, $1/\Delta x^2$, etc. The P_1 and P_2 terms are identical to the advective and diffusive terms already in our dynamic FIDI equation, Eq. (6). Inclusion of these as additional terms allows for statistical correction of simple advection and diffusive effects. P_3, which is proportional to $u^2(uu_x)$, is a type of modified advection term that might conceivably have some advantage for the representation of SGS effects. Other powers of U could also be tried and under some circumstances might be preferable. No physical justification is offered for the inclusion of P_3. Similarly P_4 is offered as a modified diffusion with a variable diffusion coefficient, U_x, simply on a trial basis.

5. Model I

Figure 2 is a typical time development with what we will refer to as Model I. This model is characterized by $k=0$ and $S(x,t,u)=S(u)$. That is, the source is a function of x and t only implicitly through variations of u. In contrast, Models II and III will contain explicit variations in space, and in space and time, respectively. Thus for Model I, since the dynamical equations are the same for all x and t, the coefficients of the P's in the STAT equation also will be independent of x and t.

For the fine-grid calculations 120 points were used along the x axis, and 15 points were used for the coarse-grid calculations. Five cases were calculated starting from the different initial conditions given by the relative amplitudes of the Fourier coefficients in Table 1.

The source function for u was calculated at each time step in a way that conserved the total kinetic energy of the flow. Denoting $u^{n+1}_{i,j+1}$ simply by u_i we used

$$\delta t S(u_i) = a(u_i - \overline{u_{i,0}}), \tag{8}$$

where the bar ($\overline{\ }$) denotes an x average. The amplitude a is independent of i and is determined at each time step by the quadratic relation

$$a^2 + 2a + (\overline{u_i^2} - \overline{u_{i0}^2})/(\overline{u_i^2} - \overline{u_i}^2) = 0, \tag{9}$$

where $u_{i,0}$ is the initial value of $u_{i,j}$. Normally $a>0$ and

TABLE 1. The relative amplitudes of cosine (A_m) and sine (B_m) components in Eq. (4) for the initial conditions of the 5 cases of Model I. The relative amplitudes of 1 for $m=1$–15 should be multiplied by 0.26.

Case	1		2		3		4		5	
m	A_m	B_m	A_m	B_m	A_m	B_m	A_m	B_m	A_m	B_m
0	0.2	—	0.2	—	0.2	—	0.2	—	0.2	—
1	0	1	1	0	0	1	1	0	1	0
2	0	1	1	0	0	1	0	1	1	0
3	0	1	1	0	1	0	1	0	0	1
4	0	1	1	0	0	1	0	1	0	1
5	0	1	1	0	0	1	1	0	1	0
6	0	1	1	0	0	1	1	0	0	1
7	0	1	1	0	1	0	1	0	0	1
8	0	1	1	0	0	1	0	1	0	1
9	0	1	1	0	0	1	1	0	1	0
10	0	1	1	0	1	0	0	1	0	1
11	0	1	1	0	1	0	0	1	1	0
12	0	1	1	0	1	0	1	0	1	0
13	0	1	1	0	0	1	1	0	1	0
14	0	1	1	0	0	1	1	0	1	0
15	0	—	1	—	1	—	1	—	0	—

Eq. (8) indicates an increment in u_i in proportion to the departure of u_i from its averaged value. This procedure restores the perturbation energy to its prescribed initial value but does not change $\overline{u_i}$.

As may be seen from the example of Fig. 2 there was a progressive dissipation in the number of fine-scale features of the initial flow. This occurred in all cases because viscosity dissipates the shorter waves more rapidly while the introduction of energy by $S(u)$ is equally effective for all waves, increasing their amplitudes in proportion to their existing amplitudes. This deterioration of the small scale structure was a non-stationary aspect of the flow that was a serious deficiency in Model I. In the later models we attempted to rectify this by designing the source function so as to continually introduce new small-scale structure.

To clarify the overall procedure the calculations of Model I will be discussed in some detail. The five cases were each integrated for 120 fine-grid time steps, thus providing 15 time levels of coarse-grid data after the space-time averaging. Each space-time average $(U_C)_{I,J}$ consisted of an 8×8 average of fine-grid values, $u_{i,j}$. These five cases therefore provided a total of $5\times15\times15$ correct values $(U_C)_{I,J}$ for the statistical study and for evaluation of the FIDI and STAT prediction models.

Starting at each coarse-grid time level after $J=2$, Eq. (6) was used to predict for 1 time step to obtain the predicted values $(U_P)_{I,J+1}$. Defining the OTS error of prediction as

$$E_{I,J+1} = (U_P)_{I,J+1} - (U_C)_{I,J+1},$$

we thus obtained $5\times15\times(15-3)=900$ values of $E_{I,J+1}$.

For the statistical analysis the finite-difference forms of $P_1 - P_4$ were calculated for each I,J. These values were then correlated with the corresponding errors, $E_{I,J+1}$. Table 2 is a correlation table representing the

TABLE 2. A correlation table for Model I giving the linear correlations between the OTS errors E and the parametric terms P_1–P_4.

	E	P_1	P_2	P_3	P_4
E	1	0.357	0.266	0.362	−0.342
P_1		1	−0.045	0.927	−0.077
P_2			1	−0.082	0.129
P_3				1	−0.609

results of this analysis. There it is clear that P_1 and P_3 might be about equally effective as advective corrections while the nonlinear diffusion term P_4 appears to be significantly better than P_2. The analysis showed that if P_3 and P_4 were used together the inclusion of P_1 and P_2 did not significantly add to the reduction of variance of $E_{I,J+1}$. Terms P_3 and P_4 together gave a multiple correlation coefficient of 0.53 and these were used in the STAT equation for Model I.

Figure 3 is an example of the predictions of the FIDI and STAT equations compared to the correct values after $T=4$, 8, and 12 time steps, having initiated the calculations at $J=3$ ($T=0$). Although both prediction equations developed sizeable errors after several time steps, from Fig. 3 it is clear that the STAT predictions gave a demonstrable improvement for the principle wave at the left of the figure. Table 3 presents the rms errors of prediction for each of the 5 cases in Model I. In each case and at each time step the STAT prediction was superior to the FIDI result.

As noted earlier, in the discussion of Fig. 2, this flow rapidly changed its character from the initial conditions. The constant regression coefficients that were used in the STAT equation therefore represented a statistical summary of dynamics that had a definite trend. To

TABLE 3. Rms errors of prediction for the 5 cases of Model I at the times $T=4$, 8, and 12 time steps.

			Case					
J	T	Method	1	2	3	4	5	All
7	4	FIDI	0.182	0.216	0.218	0.168	0.244	0.207
		STAT	0.124	0.191	0.103	0.108	0.159	0.192
11	8	FIDI	0.197	0.255	0.195	0.180	0.274	0.223
		STAT	0.153	0.171	0.129	0.143	0.235	0.170
15	12	FIDI	0.161	0.279	0.172	0.283	0.281	0.232
		STAT	0.136	0.155	0.230	0.155	0.230	0.186

partially take this known trend into account, trial calculations were made with 2 sets of regression coefficients, one set being determined and used for the first few time steps and the second set determined and used in the later stages of the prediction when the flow was somewhat smoother. A definite improvement in the overall STAT prediction was found, but the introduction of time-dependent coefficients was not pursued further with this simple model.

6. Model II

In this model our goal was to continually introduce small scales of motion through $S(x,t,u)$ to maintain a spatial variation of u with interesting SGS phenomena. For comparison with the atmosphere one might think of S as the result of a conversion from potential to kinetic energy, so it seemed desirable to make S an explicit function of x just as the generation of atmospheric energy is a function of longitude. This was accomplished by introducing Regions 1–4 along the x axis as illustrated in Fig. 4, the source regions, 1 and 3, being of equal length and treated identically. Since our calculation of S was independent of time, except

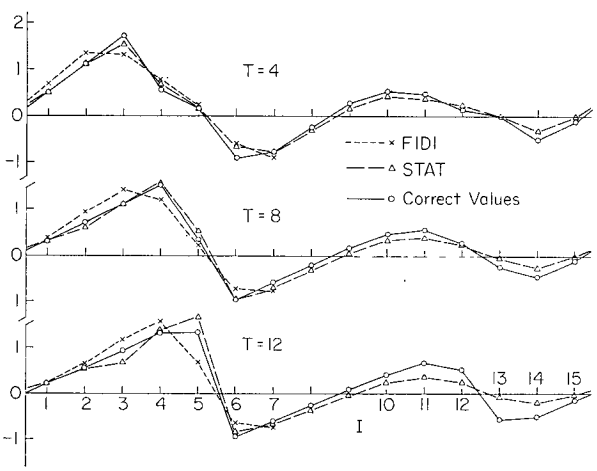

FIG. 3. A comparison of the STAT (dashed line) and FIDI (dotted line) predictions with the correct values (solid line) at times $T=4$, 8, and 12 time steps after start for Case 4 of Model I. In the region $I=7-15$ the STAT and FIDI predictions did not differ significantly.

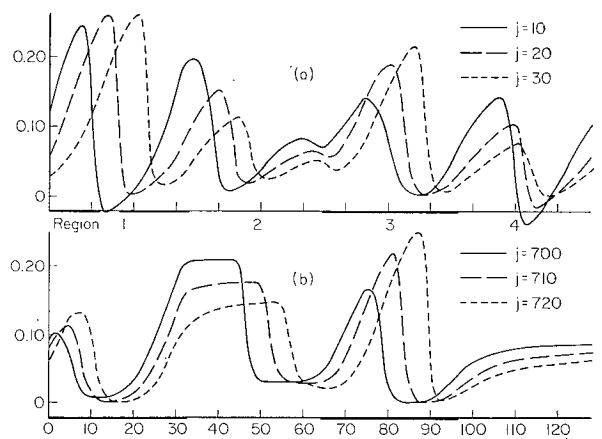

FIG. 4. Time development with Model II at intervals of 10 fine-grid time steps. (a) The development from the initial conditions. (b) A typical sequence in the quasi-periodic cycle after decay of the initial conditions. The bars along the abscissa indicate those regions in which energy was added through the source function $S(x,u)$.

implicitly through variations of u, we then had $S(x,t,u) = S(x,u)$. S was calculated and added to the prediction equations only in Regions 1 and 3.

In Model II we also introduced the damping coefficient $k=0.4$ (von Kármán's constant) to allow dissipation of the x-averaged flow, $\bar{u}$. Together with our formulation of $S(x,u)$ (as described below), this allowed an exchange of energy between $\bar{u}$ and the perturbations.

The fine-grid and coarse-grid constants used for Model II were as follows:

	Fine-grid		Coarse-grid
δx	1/128	Δx	1/16
δt	0.04	Δt	0.32
ν	0.0005	N	0.004
k	0.4	k	0.4

Thus there were 32 fine-grid points within each source or dissipation region but only 4 points for each region when using the coarse grid.

Because of the equal lengths and spacings of the source regions the overall dynamics should be identical in Regions 1 and 3 and identical in Regions 2 and 4. Accordingly, when in this model the regression coefficients were taken to be functions of I, data from each pair of I values $I=1$ and 9, 2 and 10, 3 and 11, etc., were used together to calculate the regression coefficients. These coefficients were then used for their appropriate pair of points.

From preliminary calculations we found that a specification of $S(x,u)$ similar to that used in Model I, but now applied only to Regions 1 and 3, was not satisfactory. In fact, several simple alternative forms for $S(x,u)$ led to situations in which the advective and diffusive effects were exactly balanced by the source term point by point in such a way as to lead to a stationary saw-tooth pattern of $u(x)$. To avoid these rather uninteresting stationary wave results we instituted a more complex formulation for $S(x,u)$.

The change in u at each point in the source region and after each time step was calculated from the relation

$$\delta t S(i,u_{i,j+1}^{n+1}) = u_{i,j+1}^{n+1} A_{j+1} \cos\left(\frac{8\pi i \delta x}{L} - \alpha_{j+1}\right), \quad (15)$$

where A_{j+1} is an amplitude derived to conserve the total kinetic energy and α_{j+1} is a phase angle computed separately for each source region as described below.

Equation (15) represents a simple harmonic wave of length $L/4$, the length of each source region. The phase angle of the applied wave was computed separately for each of Regions 1 and 3 by fitting a simple harmonic wave of length $L/4$ to the values of $u_{i,j+1}^{n+1}$ within each region. This method assured that changes of u were such as to amplify the dominant wave in each source region.

Figure 4a illustrates the transient initial conditions when the calculation was started from a sum of two harmonic waves with lengths $L/4$ and $L/5$. Figure 4b illustrates a typical sequence for the fine-grid calculation long after the initial transients had dissipated. Several features of the fine-grid calculation are worthy of note:

1) Individual waves could easily be followed through cyclic amplification and decay. At any time 3 waves could be identified. It is particularly interesting to note that although the forcing was by a regular 2-wave pattern of sources, the instantaneous wave pattern consisted of 3 waves. The time-averaged pattern is, of course, a 2-wave pattern.

2) The wave pattern exhibited a nearly periodic behavior with a period close to $\tau=94\delta t$. This corresponds to the average wave speed $\bar{u}_w=0.0871$. However, because of the geometrical regularity the pattern repeated itself offset by the spatial distance $L/2$ every 47 time steps.

3) The overall time-space averaged flow speed was $\bar{\bar{u}}=0.0788$, somewhat less than the wave speed. Apparently the effect of the source region was to increase the apparent wave speed during the addition of energy. This result was in marked contrast to the coarse-grid FIDI calculations, as discussed below, for which we sometimes found stationary waves.

4) The average flow $\bar{u}$ fluctuated with a standard deviation of only 1.2% of $\bar{\bar{u}}$. The 94 time-step period was not evident in the fluctuation of $\bar{u}$.

For comparison with the atmosphere we may identify one time unit with one day and the unit distance $L=1$ with the circumference of a latitude circle at 40° latitude, about 3×10^4 km. Then $\delta x=234$ km, $\delta t=0.96$ h, $\nu=5.2\times10^6$ m^2 s^{-1}, $\Delta x=1875$ km, $\Delta t=7.68$ h, and $N=41.6\times10^6$ m^2 s^{-1}. Accordingly the space-time averaged flow speed would be 27.4 m s^{-1} and the maximum speed would be about 85 m s^{-1}. Thus in a sense the fine-grid calculation might correspond in scale to present-day global circulation models, and the coarse-grid calculation would be a very crude representation of the flow.

To examine the effectiveness of evaluating and using different statistical coefficients at different I points we have also made calculations with spatially constant coefficients. The constant-coefficient model is called STAT-I and the space-variable-coefficient model is called STAT-II. Thus in the following discussion and results for Model II, we compare the FIDI, STAT-I and STAT-II predictions with the correct data. In both STAT predictions we present only those results that were obtained with the parametric terms P_1 and P_4.

The fine-grid calculation covered 1200 time steps, thus allowing the calculation of space-time averages for 150 coarse-grid time levels. Since two I points (e.g., $I=1$ and 9) were combined for statistical purposes, there were 2×149 values available for each regression equation, there being 8 such equations, one for each of the independent values of I. Of course, due to the periodicity of the flow not all of the 298 sets of data can

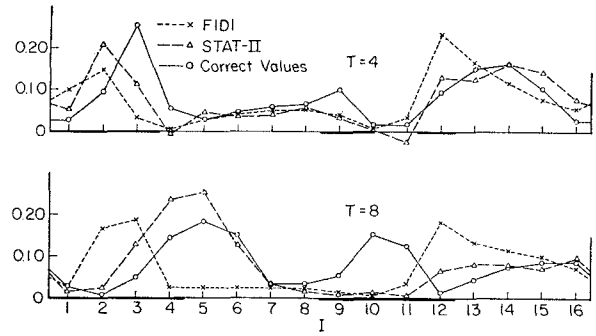

FIG. 5. Examples of the FIDI and STAT-II predictions for Model II at $T=4$ and $T=8$ time steps for Case 4.

be considered to be independent. For the STAT-I calculations 16×149 values were used for calculation of the regression coefficients. After both the constant and space-variable coefficients for the STAT-I and STAT-II predictions were determined, 6 cases were predicted starting at various phases of the overall cycle with $J=22$, 37, 57, 67, 83, and 109. For comparative purposes these starting times are referred to as $T=0$.

Figure 5 shows comparative curves of two predictions, FIDI and STAT-II, at times $T=4$ and $T=8$ for a typical case ($J=67$) in comparison with the correct values. There it is apparent that the STAT-II prediction was generally superior to the FIDI prediction, but at $T=8$ over Region 3 neither the FIDI nor the STAT-II prediction gave an indication of the growth of the wave that occurred in the correct values. Because the model requires conservation of total energy there was an overcompensation in the amplitudes over Region 1 where, apparently, conditions were more favorable for growth.

Figure 6 illustrates the rms errors of prediction for all 6 cases at the 16 I points for the three prediction methods. There it is apparent that up to $T=8$, STAT-II was superior to STAT-I, and both were significantly better than the FIDI prediction.

Figure 7 presents the average of the correlation coefficients of the 6 cases. The upper part of Fig. 7 shows the standard deviation of the correlation coefficient, σ_r, based upon all three sets of data. Arrows indicate times when each of the three curves comes within one σ_r of

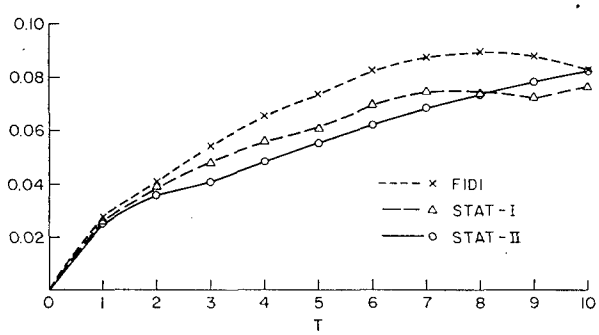

FIG. 6. Rms errors of prediction for the 6 cases of Model II.

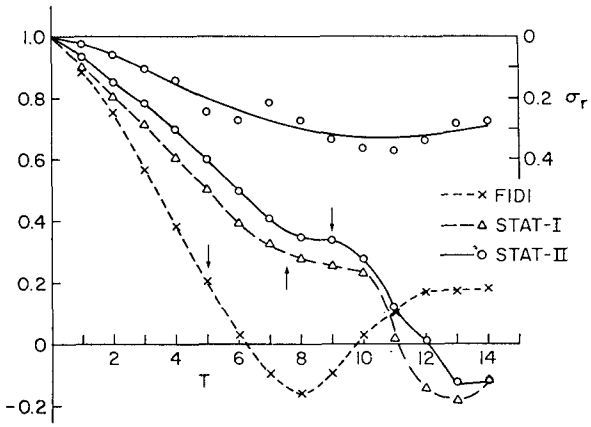

FIG. 7. Average of the prediction-correct correlation coefficients (left-hand ordinate) for the 6 cases of Model II. The upper curve (right-hand ordinate) is the standard deviation of the 18 correlation coefficients of the 3 prediction methods.

zero. Arbitrarily calling these the predictability times, T_p, we find for FIDI, $T_p=5$, for STAT-I, $T_p=7.5$ and for STAT-II, $T_p=9$. The latter time when converted to our atmospheric scale would be close to 3 days.

Of the many variations one might imagine in this problem, one would be to vary the number of iterations, n. For the data of Figs. 6 and 7, in the FIDI predictions we used $n=6$, but for calculation of the OTS errors and for the STAT predictions we used only $n=1$. For comparison we predicted one case ($J=37$) using only 1 iteration in the FIDI scheme. The step by step comparative results are given in Table 4 in terms of the rms errors. In this particular case STAT-I and STAT-II were inferior to FIDI-6 at certain times (italicized data) but were always superior to FIDI-1. These results suggest that inclusion of the statistical corrections at each time step overcame the adverse effect of using only one iteration in the STAT models. The obvious extension of the STAT models to several iterations for improved accuracy has not yet been tried.

When the FIDI predictions were examined in detail to ascertain where the maximum errors arose, it was found that after a short prediction time the waves became nearly stationary. This was found to be a direct result of the high viscosity in the coarse-grid computations, for in a series of fine-grid calculations with values

TABLE 4. A comparison of rms errors for FIDI predictions using only $n=1$ (FIDI-1) and the usual $n=6$ (FIDI-6). Only $n=1$ was used in the STAT predictions.

	T									
Model	1	2	3	4	5	6	7	8	9	10
FIDI-1	0.031	0.050	0.061	0.076	0.083	0.092	0.099	0.102	0.107	0.105
FIDI-6	0.025	0.039	0.046	0.063	0.073	0.087	0.096	0.102	0.106	0.103
STAT-I	0.021	0.038	*0.047*	*0.065*	*0.077*	*0.088*	0.082	0.061	0.048	0.052
STAT-II	0.021	*0.041*	*0.052*	*0.066*	*0.075*	0.082	0.072	0.057	0.045	0.056

TABLE 5. The relative coefficients of the additional advective term P_1 when expressed in the same finite-difference form as the normal advective term $(u^2)_x$.

Model	Coefficient of $(u^2)x$	Coefficient of $P_1(I)$ $I=$ 1,9	2,10	3,11	4,12	5,13	6,14	7,15	8,16
FIDI	1	0	0	0	0	0	0	0	0
STAT-I	1	0.85	0.85	0.85	0.85	0.85	0.85	0.85	0.85
STAT-II	1	0.94	0.75	0.70	1.41	0.84	0.70	0.53	0.59
		Regions 1 and 3				Regions 2 and 4			

$\nu=N/8$, $N/4$, $N/2$ and N it was found that the waves slowed down with increasing ν so that at $\nu=N$ the waves were nearly stationary. Thus the stationarity was a result of the high value of ν and not directly a result of the coarse grid.

The effect can be traced further to the facts that 1) the high viscosity excessively dissipates small-scale features of the flow, and 2) the input of energy is related to the pattern of flow over the source regions. Thus in this problem the coarse-grid predictions were strongly influenced by the fact that the pattern of input of energy was seriously affected by SGS patterns of flow that could not be represented in the coarse-grid case.

The above difficulties might not have been so severe with a lower value of k (less dissipation), with a greater total kinetic energy (larger Re), or with some different form for the energy input. And it is hardly to be expected that the identical problem would ever be encountered in atmospheric prediction. Nevertheless, the cause of the poor predictions of the FIDI model in this idealized flow must be considered as symptomatic of the type of problem that may arise when the resolution of the flow is decreased. For example, the generation of atmospheric kinetic energy by baroclinic processes may be quite sensitive to the phase relation between the flow patterns and the underlying surface, whether the effect of this surface be thermal or topographic. Small errors in coarse-grid predictions may then lead to large distortions of the conversion from potential to kinetic energy.

The STAT predictions were moderately successful in overcoming the predilection of the FIDI model to give a stationary wave pattern. This was mostly due to the large coefficients that were used with the P_1 term, as indicated in Table 5. There it may be seen that the coefficients of P_1 were of the same magnitude as that of the coefficient of the usual advective term $(u^2)_x$, both terms being represented in the same finite-difference form.

7. Model III

The possibility of a time variation of the C's in Eq. (7) in a situation similar to a seasonal variation was investigated in Model III. In all respects this was the same as Model II except that the total kinetic energy of the system was varied sinusoidally over the range $5-15\times10^{-3}$ with a period of $256\delta t$, 10.24 time units. This variation of the controlled KE resulted in variations of $\bar{u}$ and σ_u [the standard deviation of $u(x)$] over the approximate ranges 0.056–0.103 and 0.036–0.081, respectively. The perturbation kinetic energy $(\sigma_u^2/2)$ over 4 cycles is plotted in Fig. 8 where substantial variations from a simple periodic response are apparent.

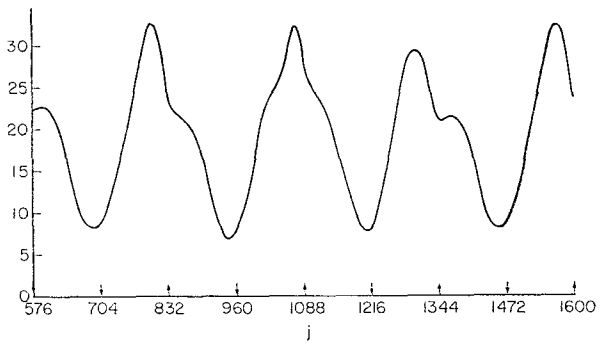

FIG. 8. Variations of the perturbation kinetic energy for Model III (fine-grid) in response to a controlled sinusoidal variation of the total energy. Arrows indicate maxima and minima of the total energy.

The period of the fundamental oscillation in coarse-grid time steps was $32\Delta t$. To avoid an unnecessarily large number of calculations, the 32 coarse-grid time steps of each cycle were divided into 8 sections of 4 steps each. Data from the 4 successive time steps of each section, for all cycles of the energy fluctuation, and for the corresponding pairs of I's were grouped together for the calculation of the regression coefficients. Since the spatial variation of the regression coefficients used in Model II was retained here, there were a total of 64 sets of coefficients to be determined.

The length of the fine-grid calculation was 4200 δt, providing 525 sets of coarse-grid data. From these data we used 16 cycles (the last 512 time steps) so that altogether there were 128 sets of data available for each regression calculation. The parametric terms used in Model III were simply P_1 and P_2, the normal advective and diffusion terms.

Figure 10 illustrates the rms errors of 8 predictions with FIDI, STAT-II (spatial variation only) and STAT-III (spatial and temporal variations). These 8 cases were started at different times in the periodic cycle of energy, and the 15 time steps of prediction illustrated in Fig. 10 are almost $\frac{1}{2}$ of the total period, $32\Delta t$. The rms errors show that over the first 6 time steps there was no substantial improvement obtained by allowing time variation of the regression coefficients. While STAT-III appears to be superior after $T=6$ it is doubtful that this result is statistically significant.

8. Conclusions

These results indicate that at least in this simple and well-controlled system the proposed method is capable

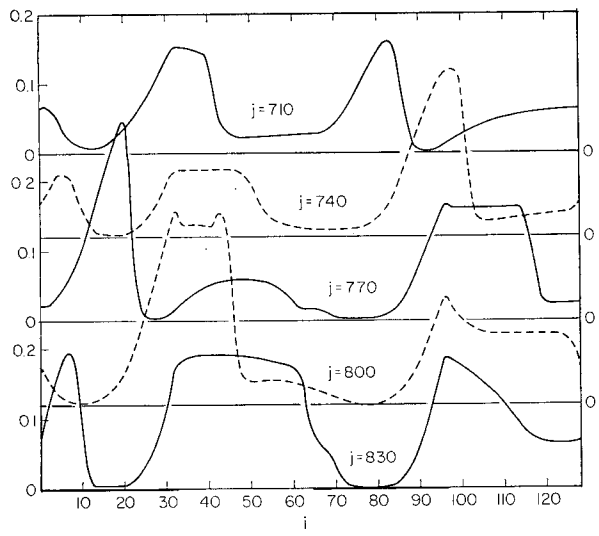

FIG. 9. The temporal development over approximately one-half cycle of the variation of total kinetic energy for Model III. See Fig. 8 for the corresponding variation of the perturbation kinetic energy.

of producing substantial improvements over normal coarse-grid predictions. The method is, basically, to add statistically determined corrections to the prediction at the end of each time step. The effects of these corrections then are carried through the subsequent steps.

This procedure differs substantially from attempts to apply statistical corrections at the termination of a prediction (say after 12 h of atmospheric prediction) or after many time steps. The nonlinear effects of errors of prediction are cumulative in time and spread their influence over larger and larger areas, propagating with the fastest wave speed allowed by the system and by diffusion. Under such circumstances it seems unlikely that the cumulative errors after many time steps can be statistically related to the large-scale flow variables by linear regression unless there has been rather little change in this flow. Clearly, the statistical correction of errors at each time step has the potential of overcoming the difficulties cited above, but it may introduce other problems of a more serious nature, and it is the goal of this research to see if these can be successfully overcome.

The requirement of computational stability of the system undoubtedly is one of the more serious problems. In the present study stability is guaranteed by control of the total energy at the end of each time step. This constraint would not be realistic in the atmosphere, but similar controls might be introduced at convenient points in the numerical procedure in such a way as to allow the flexibility that a natural system may require.

It has been pointed out to the authors that the accuracy of the fine-grid calculation may be in question. In the context of this study this is not a concern since we regard the finite-difference equations, including their given space and time increments and the method of solution, as the model system. The only uncertainties in the model system then are round-off errors of the computer. Thus, the philosophy is that we have some coarse-grid data from some dynamical system for which we believe (or assume) that we know the physical equations. To arrive at a viable prediction scheme we replace our assumed physical equations with a set of approximate coarse-grid difference equations or any other suitable set of equations (perhaps in spectral form) that can be solved for future values of the coarse-grid variables. Realizing: 1) that the coarse-grid difference equations are approximations, 2) that the coarse-grid data with which we initiate and test our predictions mask SGS phenomena and may contain errors, and 3) that there may be physical processes in the basic model system that are not included in our coarse-grid model, we attempt to partially remedy these deficiencies by the addition of statistical corrections. In this context it is apparent that the accuracy of the fine-grid solution, accuracy in the sense of having started with some differential equations that are being approximated, is not a relevant problem.

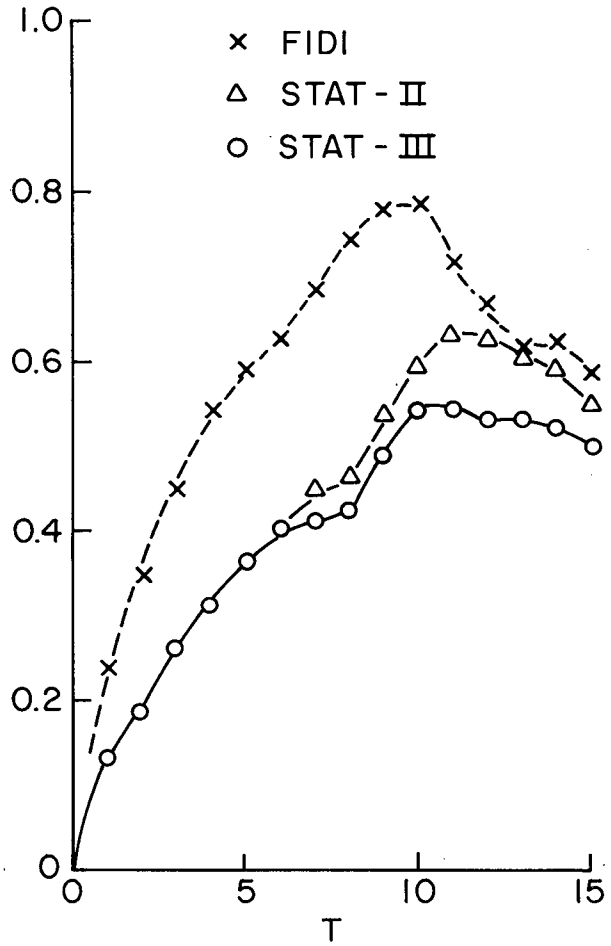

FIG. 10. The rms errors of prediction for Model III.

Although we have tested our corrections with the same body of data that was used to calculate the corrections, this procedure is justified because: first, the statistical coefficients were based upon the errors after only one time step whereas the verifications were made after many time steps during which the errors accumulated and compounded; second, for these relatively simple examples "independent" test cases would almost exactly reproduce the original data and would add nothing new unless new dynamics were introduced. The introduction of fundamentally different dynamics would of course require the calculation of new correction terms.

Because of the many possible variants of the proposed method, in general approach as well as in detail, we regard the present one-dimensional study only as a first step in an extended investigation of these possibilities. Studies of model two-dimensional flows and real fluid systems are now under consideration.

REFERENCES

Benton, E. R., and G. W. Platzman, 1972: A table of solutions of the one-dimensional Burgers equation. *Quart. Appl. Math.*, **30**, 195–212.

Burgers, J. M., 1974: *The Non-Linear Diffusion Equation.* D. Reidel, 174 pp.

Crowley, W. P., 1970: A numerical model for viscous, free-surface, barotropic wind driven ocean circulations. *J. Comp. Phys.*, **5**, 139–168.

Deardorff, J. W., 1970: A three-dimensional investigation of the idealized planetary boundary layer. *Geophys. Fluid Dyn.*, **1**, 377–410.

Leith, C. E., 1969: Two-dimensional eddy viscosity coefficients. *Proceedings, WMO/IUGG Symposium on Numerical Weather Prediction*, Tokyo, Japan Meteor. Agency.